Formation of nanocomposite platinum catalysts on porous silicon

N. A. Yashtulov,[a] S. S. Gavrin,[a] V. P. Bondarenko,[b] K. I. Kholostov,[b] A. A. Revina,[c] and V. R. Flid[a]*

[a] *M. V. Lomonosov Moscow State Academy of Fine Chemical Technology, 86 prosp. Vernadskogo, 119571 Moscow, Russian Federation. Fax: +7 (495) 434 7111. E-mail: YashtulovNA@rambler.ru*

[b] *Belarusian State University of Informatics and Radioelectronics, 6 ul. P. Brovki, 220013 Minsk, Belarus. Fax: +375 (17) 293 8843. E-mail: kholostov@gmail.com*

[c] *A. N. Frumkin Institute of Physical Chemistry and Electrochemistry, Russian Academy of Sciences, 31 Leninsky prosp., 119991 Moscow, Russian Federation. Fax: +7 (495) 955 4017*

Platinum nanoparticles supported on porous silicon were synthesized by radiation-chemical reduction in solutions of reverse micelles. The Pt nanoparticles obtained are electron-deficient. The degree of porosity, conductivity type, pore geometry of the silicon matrix, and precursor parameters affect the size, shape, and charge state of the platinum catalysts.

Key words: platinum nanocomposites, porous silicon, atomic force microscopy, X-ray photoelectron microscopy, specific adsorption, electrocatalysis.

Platinum and platinum-based composites are considered to be the best catalysts of oxygen reduction reactions (ORR) and hydrogen oxidation reactions (HOR) that occur in electrochemical power generators. It was shown in a series of our works[1—4] and other publications[5—8] that nanoparticles of platinum metals and silver supported on porous silicon (PS) and carbon nanotubes are efficient electrocatalysts for fuel cells.

Synthesis of metal nanoparticles in solutions of reverse micelles followed by their subsequent adsorption on porous supports is a promising method for nanoelectrocatalyst formation.[2—4] Reverse micelles are spherical microdroplets of water (pools) stabilized by surfactants (Surf) in an organic solvent. The molar ratio $\omega_0 = [H_2O]/[Surf]$ defined as the solubilization coefficient determines the size of formed metal nanoparticles during the reduction of their ions in water pools. An increase in this ratio favors the formation of larger nanoparticles.

There are few published data describing how the electrocatalytic activity of nanoparticles deposited on the PS surface is influenced by their physicochemical properties.[2—6] Therefore, it is of interest to reveal the character of the metal—PS interaction, morphology of supported particles, charge state of the surface, and possibility of formation of new phases and active sites. Information of this kind makes it possible to better understand specific features of the mechanism of electrocatalytic reactions.

The formation of catalytic composites involving Pt nanoparticles can result in the appearance of electron-deficient $Pt^{\delta+}$ atoms and the electron density redistribution at the Pt/semiconductor interface. In addition, chemisorption of metal nanoparticles on the support will lead, probably, to the formation of chemical compounds between the catalyst and supporting matrix.[9,10] On the one hand, it is considered[11] that the adhesion of Pt nanoparticles on the silicon support is weak because of the low surface energy of interaction between Pt and Si. On the other hand, it is elucidated that new crystalline phases based on Pt, Re, Ru, and Mo are formed[12,13] during the formation of supported metal catalysts with high degree of dispersity. The high electrocatalytic activity of the nanocatalyst Pt_3Sn was shown[14] in the reaction of EtOH oxidation. Surface intermetallic compounds Pt_3Co, Pt_3CoCr, and Pt_xNi are active in the ORR.[15,16]

To solve many controversial questions about the interaction of metal particles with the support, it is important to know the state of these particles on the surface.

Measurements of surface potential are usually used to determine the sign of charge of adsorbed catalytic nanoparticles. This characteristic can be used to get insight into the nature of nanoparticles.[9] It was shown that palladium nanoparticles on PS have lower values of surface potential than those on monocrystalline silicon[4] and possess excessive positive charge δ+. The presence of nanocomposites $Pd^{\delta+}$/PS can favor the catalytic decomposition of CO and electrooxidation of H_2.

The purpose of the present work is to obtain data on the influence of the type of conductivity, degree of porosity, pore geometry of silicon, and precursor parameters on the surface potential, charge, and phase state of Pt nano-

Published in Russian in *Izvestiya Akademii Nauk. Seriya Khimicheskaya,* No. 3, pp. 425—430, March, 2011.

1066-5285/11/6003-434

particles. It was also of interest to evaluate the influence of the nature of the Pt/PS nanocomposites on specific features of the mechanism of rate-determining steps of the ORR and HOR.

Experimental

The surface potential of porous silicon samples was measured with an NTegra Prima atomic force microscope (NT-MDT) using the Kelvin probe method.[17] In this method, we used the procedure of double scanning: the surface topography was determined during the first scanning of the probe above the studied surface, and the electric interaction of the probe with the sample at the fixed distance between the probe and sample (10 nm) was measured during the second scanning. The frequency detection of the signal made it possible to study the distribution of surface potential (U_s).

Platinum nanoparticles were synthesized by the radiation-chemical reduction of ions Pt^{4+} under anaerobic conditions in solutions of reverse micelles followed by nanoparticle adsorption on the PS surface according to the procedure described earlier.[18,19] Sodium bis(2-ethylhexyl)sulfosuccinate (AOT, $C_{20}H_{37}SO_7Na$, 99%, Sigma) was used as the surfactant. For the synthesis we used H_2PtCl_6 (reagent grade). The solutions prepared were sealed and γ-irradiation with ^{60}Co was carried out on a RKhM-γ-20 setup. The molar ratio water : AOT was varied from 1.5 to 5, which corresponds to the solubilization coefficient $\omega_0 = [H_2O]/[AOT] = 1.5—5$.

Samples of porous silicon with conductivity of the n- and p-types and the degree of porosity (P) from 40 to 78% were synthesized using standard procedures.[2,3] Plates of PS were subjected to anodic electrochemical etching in aqueous-ethanol solutions of HF. For the galvanostatic anodation regime, the current density was 20—100 mA cm^{-2}. As a result, plates were obtained, whose porous layers are 1 μm thick, the pore diameter of the channels for PS of the n-type is 20—50 nm, and that for PS of the p-type was 5—20 nm.

The X-ray photoelectron spectra (XPS) of Pt nanoparticles adsorbed on PS were recorded on a PHI 5500 ESCA spectrometer (Perkin—Elmer). Monochromatized Al-Kα radiation (hv = = 1253.6 eV) was used to excite photoemission. High-resolution spectra were recorded at a transmission energy of the analyzer of 29.35 eV and a level of collection density of 0.125 eV increment^{-1}. According to the XPS data, the accuracy of estimation of the content of adsorbed Pt nanoparticles is 1—2%.[9]

Absorption spectra in the wavelength range from 190 to 1000 nm were measured on a UV-3101 PC spectrophotometer (Shimadzu, Japan) at room temperature. A 0.15 M AOT—isooctane solution was used as reference. The content of adsorbed Pt nanoparticles was estimated spectrophotometrically using calibration by the amount of H_2PtCl_6 in the initial solutions at the fixed value of ω_0. The accuracy of experimental data was 5—7%.

The pore morphology of the silicon samples was studied by scanning electron microscopy (SEM) on a JSM-7401F instrument (JEOL, Japan) with an INCA analyzer (Oxford Instruments, England).

Results and Discussion

The plots of the surface potential of PS and Pt/PS nanocomposites obtained from solutions with $\omega_0 = 5$ for conductivity of the n- and p-types *vs* degree of porosity of the silicon matrix are shown in Fig. 1. For nonporous silicon ($P = 0\%$) with conductivity of the n- and p-types, the presence of adsorbed platinum nanoparticles results in an increase in the surface potential, which is explained by an increase in the electron conductivity. The values of U_s are almost the same for the PS samples of the n- and p-types. This indicates that the Pt nanoparticles make the main contribution to the total electric conductivity. An increase in the degree of porosity of silicon ($P > 40\%$) without Pt nanoparticles is accompanied by the migration of charge carriers deep into the pores and by a decrease in U_s (see curves *1* and *2*). In such open surface layers electric conductivity is considered to occur by jumps of charge carriers between crystallites.[20]

The character of changing the surface potential for the Pt/PS nanocomposites at $P > 40\%$ (see curves *3* and *4*) differs from the dependences obtained for PS in the absence of Pt (see curves *1* and *2*). First, with the introduction of Pt nanoparticles into the nanoporous PS matrix the value of U_s does not increase as in the case of nonporous silicon, but decreases considerably. A comparison of the data for the silicon matrices of the n- and p-types shows that at the same degree of porosity the values of U_s for PS containing Pt are lower than the values for the PS samples without Pt. Second, for PS of the n-type with Pt the values of U_s are lower than those for PS of the p-type with Pt (see curves *3* and *4*). This means that the introduction of Pt into PS results in the appearance of excessive positive charge δ+, on the surface whose value on PS of the n-type is higher than that on PS of the p-type.[9] Third, in the range $P = 40—80\%$ the degree of porosity exerts a weak effect on the change in U_s for both the n- (see curve *3*) and p-type (see curve *4*).

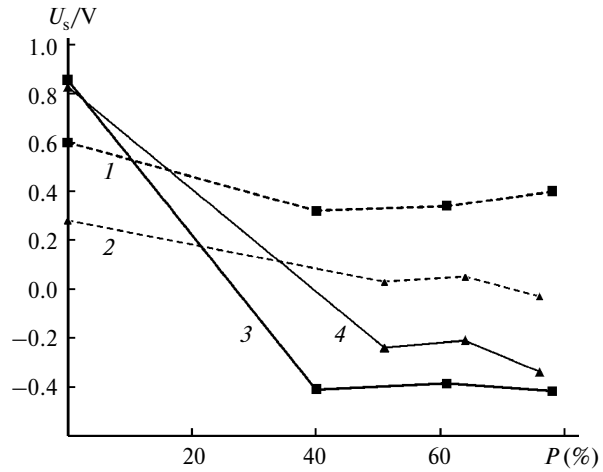

Fig. 1. Potential of PS (U_s) *vs* degree of porosity (P) at the degree of solubilization $\omega_0 = 5$ for the PS samples with conductivity of n- (*1*) and p-types (*2*) and for the platinum nanocomposites with PS with conductivity of the n- (*3*) and p-types (*4*).

The increase in U_s on the nonporous silicon surface ($P = 0\%$) with platinum nanoparticles is due to the fact that adsorbed Pt nanoparticles possess the metal-type conductivity. Similar results are usually observed in studies of nonporous materials with low electric conductivity. Under these conditions, closed metal structures are formed on the surface of such nonporous materials.[21] The adsorption capacity of PS with the specific surface above 400 $m^2 g^{-1}$ is substantially higher than that of nonporous silicon.[20,21] Nevertheless, the value of U_s for Pt-containing PS composites is lower than that for nonporous silicon with Pt. It cannot be excluded that differences in the values of surface potential for PS with Pt and nonporous silicon are due to a stronger interaction of the Pt nanoparticles with the PS surface to form chemisorbed composites Pt/PS. As a result, the fraction of metal Pt nanoparticles decreases.

The examples illustrating the influence of the degree of solubilization on the values of U_s for the Pt/PS composites of the n- and p-types of conductivity are presented in Table 1. The surface potential decreases with an increase in ω_0 for the nanocomposites with any type of PS conductivity. When ω_0 increases from 1.5 to 5, the value of U_s for the conductors of the n-type decreases more strongly than for the p-type conductors. Therefore, solubilization decreases the electric conductivity on PS of the n-type more strongly than on the p-type PS and the PS surface of the n-type is characterized by a higher positive charge $\delta+$.[9] The maximum change in the surface potential occurs for adsorption from solutions of the precursor with $\omega_0 = 5$. These solutions have maximum sizes of the water pool of micelles and fractions with an increased content of large Pt nanoparticles are deposited on PS from them during adsorption.[2,3,12]

Spectrophotometric analysis of reverse-micelle solutions of PT during nanocomposite formation was carried out to reveal the nature of the adsorption capacity of PS of the n- and p-types. In the optical absorption spectra of solutions of reverse micelles, the Pt nanoparticles are characterized by the intense band of plasmon absorption at 230—280 nm. Its position and width depend mainly on the particle sizes and shape. The values of wavelengths of maxima and width at the half-height at various ω_0 are listed in Table 2. With an increase in ω_0 from 1.5 to 5, the peak maximum undergoes the bathochromic shift with the substantial broadening of the absorption band (by ~2 times). Both the increase and broadening of the absorption wavelength can indicate that the fraction of larger nanoparticles increases with ω_0 and the shape of the larger nanoparticles possibly deviates from the spherical pattern.[21]

Table 2. Characteristics of the absorption spectra of the Pt nanoparticles in solutions of reverse micelles (absorption maxima (λ) and width at the half-height (Δ)) at various ω_0

ω_0	λ	Δ
	nm	
1.5	244	36
3.0	255	53
5.0	261	71

The data on the change in the integral intensity of characteristic bands of plasmon absorption of the Pt nanoparticles obtained by their adsorption on PS of the n- and p-type for 72 h are presented in Table 3. The integral intensity remains almost unchanged for longer adsorption times. The integral intensity is proportional to the amount of nanoparticles in the sample and can serve as an indicator of the concentration of adsorbed Pt nanoparticles. According to the data in Table 3, the amount of Pt nanoparticles adsorbed on PS of the n- and p-types depends weakly on ω_0. At any values of ω_0 the samples of the n-type adsorb more platinum than the p-type samples. Since the concentration of nanoparticles in the pools is the same,[1,2,4,12] the amount of Pt nanoparticles in the water pool of reverse micelles increases with an increase in the pool diameter and, hence, the solubilization coefficient. Therefore, the close content of Pt adsorbed on PS at different values of ω_0 can be explained assuming that the adsorption affinity of platinum nanoparticles increases with a decrease in their size.

As mentioned above (see Table 1), for the adsorption of Pt on PS, the surface potential decreases considerably with an increase in the degree of solubilization from 1.5 to 5. At the same time, according to the optical spectral data (see Table 3), the amount of adsorbed Pt nanoparticles on PS remains almost unchanged as the degree of solu-

Table 1. Surface potential (U_s) of the Pt nanocomposites on PS at various degrees of solubilization (ω_0)

Conductivity type (porosity P (%))	U_s/V		
	$\omega_0 = 1.5$	$\omega_0 = 3$	$\omega_0 = 5$
n (40)	0.43	−0.08	−0.41
p (51)	0.23	0.02	−0.24

Table 3. Change in the total integral absorption intensity of solutions of the Pt nanoparticles due to adsorption on PS

Conductivity type (P (%))	Intensity change (%)		
	$\omega_0 = 1.5$	$\omega_0 = 3$	$\omega_0 = 5$
n (40)	14.5	15.4	14.9
p (51)	11.8	13.9	10.6

bilization decreases. Probably, the main influence on the surface potential is made not by the amount adsorbed but the character of interaction between the adsorbent (PS) and adsorbate nanoparticles, which depends on the type of conductivity of PS and the sizes and shape of Pt nanoparticles and PS pores.

The silicon samples with conductivity of the n- and p-types and the same degree of porosity obtained from micelles with $\omega_0 = 5$ were studied by XPS in order to estimate the charge state and content of the Pt nanocomposites on the PS surface. The fragments of the Pt (4f) high-resolution spectra with nonlinear approximation are shown in Fig. 2. The Pt XPS spectra for the PS samples with conductivity of the n- and p-types differ noticeably in the shape of the curves. The platinum spectrum for the samples of the n-type is presented by two doublets: the first doublet of line $4f_{7/2}$ lies at 71.9±0.1 eV, and the second doublet lies at 73.8±0.1 eV. According to the reference data,[22] the bond energy $E_b(4f_{7/2})$ in pure Pt and in its compounds with Si and O changes as follows:

Compound	$E_b(4f_{7/2})$/eV
Pt	71.2
Pt_2Si	72.5
PtSi	73.0
PtO	73.8—74.2
PtO_2	74.6—75.0

An analysis of the spectral pattern suggests that the Pt atoms in the nanoparticles adsorbed on PS of the n-type differ in the charge state ($0 < \delta \leq +2$). Some of them probably form Pt—O bonds whereas other Pt atoms are bonded to silicon forming silicide Pt_2Si.

The platinum spectrum in the PS samples of the p-type is presented by one doublet of peaks $4f_{5/2}$ and $4f_{7/2}$ caused by the spin-orbital splitting of the 4f-level. Line $4f_{7/2}$ lies at 72.5±0.1 eV. It can be concluded that for the Pt nanocomposites on PS of the p-type all Pt atoms are equivalent in charge state δ. In these catalysts the chemical bonds of Pt with oxygen are absent and silicon is bound to platinum due to bonds in silicide Pt_2Si.

Thus, electron-deficient platinum nanoparticles $Pt^{\delta+}$ are formed on the PS surface due to chemisorption.

The results of XPS allow one to calculate the content of Pt nanoparticles on the PS surface of the n- and p-types, which were deposited at $\omega_0 = 5$. Somewhat larger amount of platinum is adsorbed on the n-type surface compared to the surface of the p-type. A comparison of the data obtained by the study of Pt nanoparticle adsorption on PS by XPS and spectrophotometry shows that photoelectron spectroscopy gives lower values of the adsorbed platinum content. However, the data of both methods indicate that the content of platinum nanoparticles on the surface of the n-type is larger than on the p-type surface. The Kα-Al radiation used in this work provides information about the near-surface layer with the depth not more than 2—3 nm.

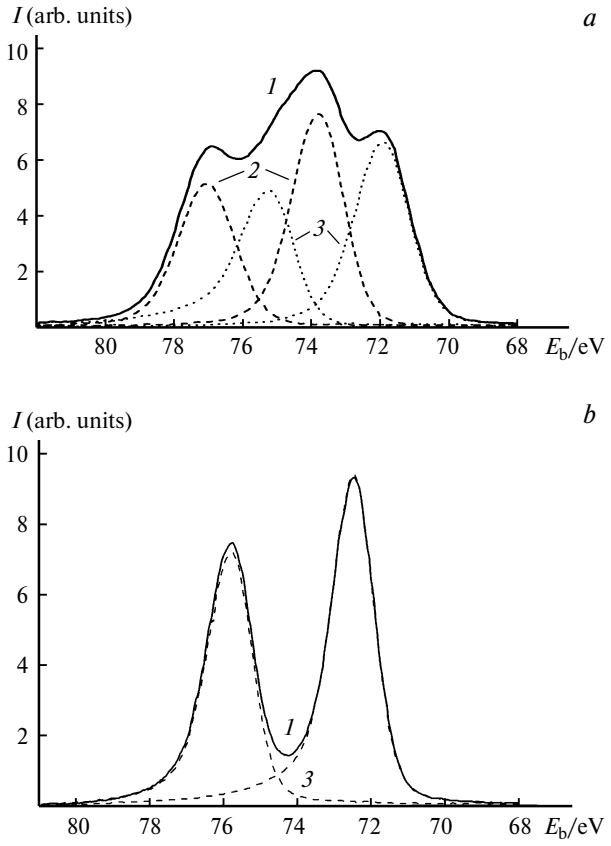

Fig. 2. X-ray photoelectron Pt spectra ($4f_{5/2}$ and $4f_{7/2}$) of the Pt nanocomposite with conductivity of the n- (*a*) and p-types (*b*): general view (*1*), Pt^{2+} (*2*), and $Pt^{\delta+}$ (*3*).

The n-type PS with the pore sizes 20—50 nm was used for the formation of Pt nanocomposites, and PS of the p-type has a smaller pore sizes (5—20 nm). The SEM image of the chip of the n-type PS sample with $P = 61\%$ is presented in Fig. 3. The difference in the content of the Pt nanoparticles revealed by the data of XPS and spectrophotometry can be explained by the different depth of penetration of Pt nanoparticles into pores of the PS matrix. In contrast to the p-type PS, porous silicon of the n-type contains larger pores, and platinum is adsorbed in increased amounts both in the whole volume of samples and in the near-surface layer of the silicon matrix (Table 4). Adsorption area inside the pore depth of PS of the n-type with a diameter of 20—50 nm is accessible for almost all fractions of micellar solutions with $\omega_0 = 1.5$—5 and sizes of Pt nanoparticles of 2—14 nm.[2—4] For PS of the p-type with smaller nanopores (5—20 nm), Pt nanoparticles are mainly adsorbed, most likely, in the near-surface layer of the silicon matrix rather than inside the pores. According to the data of spectrophotometry (see Table 3) and XPS (see Table 4), the fraction of particles adsorbed in the near-surface layer of the silicon matrix makes up 65% of the total amount of adsorbed platinum for silicon of the

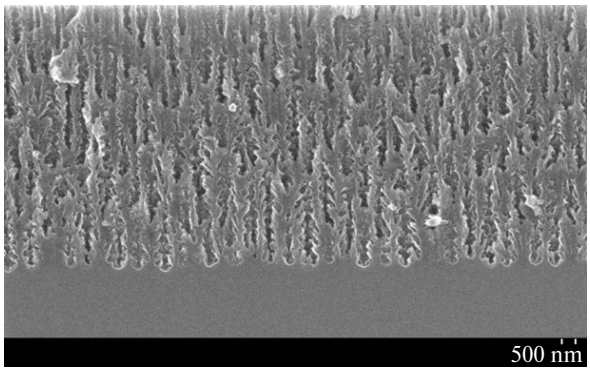

Fig. 3. SEM image of the chip of the PS sample with conductivity of the n-type and degree of porosity $P = 61\%$.

n-type and up to 90% for PS of the p-type. For adsorption in the pore depth of the matrix it is necessary that the size of the precursor nanoparticles would not exceed the cross-section of nanopores.

Although a larger amount of platinum is adsorbed on the n-type PS than on PS of the p-type, the change in porosity and the degree of solubilization exert a considerably stronger effect on the decrease in the surface potential for the samples of the n-type (see Fig. 1 and Table 1). These data can be explained by the formation of nanocomposites Pt/PS ($Pt^{\delta+}$/Pt—Si), resulting in the positive charge delocalization (δ+) on the surface and a decrease in the value of surface potential.[9] According to the XPS data, composites of the n-type contain more electron-deficient particles with $\delta = +2$ than the p-type composites (see Fig. 2). Therefore, the degree of polarization of the Pt nanocomposites on PS of the n-type is higher than that for the p-type. Similar effect can be due to the fact that local energy traps[20] on the surface of broader pores of PS of the n-type capture charge carriers (electrons of Pt nanoparticles) more intensely than traps on the surface of narrower pores of the p-type PS.

The transfer of an electron density from the metal catalyst to the electron-deficient supporting matrix should be taken into account in order to reconsider the mechanism of heterogeneous catalytic reactions. The increase in the catalytic activity of supported metals can be related to the appearance of electron-deficient nanostructures.[9,21] The catalytic effect of platinum in the most important processes of hydrogen oxidation and oxygen reduction in electrochemical generators includes the formation of complexes with H_2 and O_2, respectively. The rate-determining step of electrocatalytic hydrogen oxidation on platinum metals is the dissociative decomposition of adsorbed H_2. Similarly to the nanocomposites $Pd^{\delta+}$ on PS (see Ref. 4), the electron-deficient $Pt^{\delta+}$ nanocomposites on PS can initiate the heterolytic decomposition of an H_2 molecule with the formation of hydrated ions H^+ according to the Heyrovský—Volmer mechanism[23]

$$Pt^{\delta+} + H_2 \longrightarrow [PtH^{\delta-1}] + H^+, \quad (1a)$$

$$[Pt^{\delta-1}] \longrightarrow Pt^{\delta+} + H^+ + 2\,e^-. \quad (1b)$$

For platinum nanoparticles in the ORR, we confirmed[23] the possibility of both two- and four-electron mechanism of catalysis. The rate-determining steps of electrocatalytic oxygen reduction on platinum is the one-electron oxidation of O_2 and oxidation—decomposition of H_2O_2 *via* the two-electron mechanism.[23,24] The presence of the $Pt^{\delta+}$ nanocomposites on PS probably favors an increase in the rates of the rate-determining steps

$$Pt^{\delta+} + O_2 \longrightarrow [Pt^{\delta-1}—O^-—O^+] + e^- \longrightarrow Pt^{\delta+} + O_2^-, \quad (2a)$$

$$Pt^{\delta+} + H_2O_2 \longrightarrow [Pt^{\delta+}—O^-—O^+] + e^- \longrightarrow Pt^{\delta+} + HO^- + HO^{\cdot}. \quad (2b)$$

The results obtained indicate that electron-deficient platinum nanocomposites capable of decreasing the surface potential are formed on the PS surface. It was found that more platinum nanoparticles are adsorbed on PS of the n-type than on the p-type PS, and these particles are more strongly polarized. The charge state, concentration, size, and shape of the platinum nanocomposites depend on a combination of the size of silicon nanopores and platinum nanoparticles in the initial solutions.

Table 4. Content of Pt determined by X-ray photoelectron spectroscopy for the Pt nanocomposites on PS with conductivity of the n- and p-types

Conductivity type (P (%))	$E_b(4f_{7/2})$/eV		C* (%)	$Pt^{\delta+}/(Pt^0 + Pt^{\delta+})$ (%)
	Pt^0	$Pt^{\delta+}$		
n (40)	71.2	71.9, 73.8	9.7—12.4	78
p (51)	71.2	72.5	7.0—9.3	>90

* C is the content of Pt and $Pt^{\delta+}$.

This work was financially supported by the Russian Foundation for Basic Research (Project Nos 09-08-00547 and 09-08-00758).

References

1. N. A. Yashtulov, S. S. Gavrin, D. A. Tanasyuk, A. A. Revina, *Zh. Neorg. Khim.*, 2010, **55**, 210 [*Russ. J. Inorg. Chem.* (*Engl. Transl.*), 2010, **55**, 174].
2. N. A. Yashtulov, S. S. Gavrin, V. A. Labunov, A. A. Revina, *Nano- i Mikrosistemnaya Tekhnika* [*Nano- and Microsystem Techniques*], 2008, **8**, 20 (in Russian).
3. N. A. Yashtulov, S. S. Gavrin, *Nanoindustriya* [*Nanoindustry*], 2007, **2**, 36 (in Russian).

4. N. A. Yashtulov, S. S. Gavrin, A. A. Revina, V. R. Flid, *Izv. Akad. Nauk*, *Ser. Khim.*, 2010, 1450 [*Russ. Chem. Bull.*, *Int. Ed.*, 2010, **59**, 1482].
5. G. S. Mishra, S. Sinha, *Catal. Lett.*, 2008, **125**, 139.
6. H. Lee, S. E. Habas, G. A. Somorjai, P. Yang, *J. Am. Chem. Soc.*, 2008, **130**, 5406.
7. M. R. Tarasevich, V. A. Bogdanovskaya, B. M. Grafov, N. M. Zagudaeva, K. V. Rybalka, A. V. Kapistin, Yu. A. Kolbanovskii, *Elektrokhimiya*, 2005, **41**, 840 [*Russ. J. Electrochem.* (*Engl. Transl.*), 2005, **41**, 746].
8. J. S. Wainright, R. F. Savinell, C. C. Liu, M. Litt, *Electrochim. Acta*, 2003, **20—22**, 2869.
9. O. V. Krylov, *Geterogennyi kataliz* [*Heterogeneous Catalysis*], Akademkniga, Moscow, 2004, 679 pp. (in Russian).
10. *Physico-Chemical Phenomena in Thin Films and Solid Surfaces*, Eds L. I. Trakhtenberg, S. H. Lin, O. J. Ilegbusi, Academic Press, Amsterdam, 2007, **34**, 804 pp.
11. C. Feng, P. C. H. Chan, I.-Ming Hsing, *Electrochem. Commun.*, 2007, **9**, 89.
12. F. Vigier, C. Coutanceau, A. Perrard, E. M. Belgsir, C. Lamy, *J. Appl. Electrochem.*, 2004, **34**, 439.
13. N. Kristian, X. Wang, *Electrochem. Commun.*, 2008, **10**, 12.
14. V. A. Grinberg, N. A. Maiorova, A. A. Pasynskii, *Elektrokhimiya*, 2009, **45**, 1427 [*Russ. J. Electrochem.* (*Engl. Transl.*), 2009, **45**, 1321].
15. A. Yu. Tsivadze, *Tez. dokl. Mezhdunar. simp. po vodorodnoi energetike* [*Proc. Intern. Symp. Hydrogen Power Engineering*] *(Moscow, December 1—2, 2009)*, Moscow, 2009, 74 (in Russian).
16. V. E. Guterman, I. N. Leont´ev, Yu. V. Kabirov, E. P. Fokin, T. A. Lastovina, S. V. Belenov, N. A. Prutsakova, *Tez. dokl. Mezhdunar. simp. po vodorodnoi energetike* [*Proc. Intern. Symp. Hydrogen Power Engineering*] *(Moscow, December 1—2, 2009)*, Moscow, 2009, 48 (in Russian).
17. V. L. Mironov, *Osnovy skaniruyushchei elektronnoi mikroskopii* [*Fundamentals of Scanning Electron Microscopy*], Tekhnosfera, Moscow, 2004, 144 pp. (in Russian).
18. A. A. Revina, A. N. Kezikov, E. V. Alekseev, E. B. Khailova, V. V. Volod´ko, *Nanotekhnika* [*Nanotechnology*], 2005, **4**, 105 (in Russian).
19. A. A. Revina, A. N. Kezikov, O. G. Larionov, V. T. Dubenchuk, *Zh. Ros. Khim. o-va im. D. I. Mendeleeva*, 2006, **4**, 55 [*Mendeleev Chem. J.* (*Engl. Transl.*), 2006, **4**, 55].
20. S. P. Zimin, *Fizika i Tekhnika Poluprovodnikov* [*Physics and Technology of Semiconductors*], 2000, **34**, 359 (in Russian).
21. I. P. Suzdalev, *Nanotekhnologiya: fiziko-khimiya nanoklasterov, nanostruktur i nanomaterialov* [*Nanotechnology: Physicochemistry of Nanostructures and Nanomaterials*], KomKniga, Moscow, 2005, 592 pp. (in Russian).
22. J. F. Moulder, W. F. Stickle, P. E. Sobol, K. D. Bomben, *Handbook of X-ray Photoelectron Spectroscopy*, Ed. J. Chastain, Perkin-Elmer Corp., Eden Prairie, MN, USA, 1992, 261 pp.
23. B. B. Damaskin, O. A. Petrii, T. A. Tsirlina, *Elektrokhimiya* [*Electrochemistry*], Khimiya, Moscow, 2001, 624 pp. (in Russian).
24. N. A. Yashtulov, A. A. Revina, V. R. Flid, *Izv. Akad. Nauk*, *Ser. Khim.*, 2010, 1456 [*Russ. Chem. Bull., Int. Ed.*, 2010, **59**, 1488].

Received October 14, 2010;
in revised form March 23, 2011